Inorg. Chem. **2005**, *44*, 5789–5797

Borderline Class II/III Ligand-Centered Mixed Valency in a Porphyrinic Molecular Rectangle

Peter H. Dinolfo,[†] Suk Joong Lee,[†] Veaceslav Coropceanu,[‡] Jean-Luc Brédas,[‡] and Joseph T. Hupp*[,†]

Department of Chemistry, Northwestern University, Evanston, Illinois 60208-3113, and School of Chemistry and Biochemistry, Georgia Institute of Technology, Atlanta, Georgia 30332-0400

Received May 23, 2005

A molecular rectangle of the form $([Re(CO)_3]_2BiBzIm)_2$-μ,μ'-$(LL)_2$, where BiBzIm is 2,2′-bisbenzimidazolate and LL are cofacially aligned [5,15-bis(4-ethynylpyridyl)-10,20-bis(*n*-hexyl)-porphyrinato]zinc ligands, has been examined via electrochemical, spectroelectrochemical, and electronic Stark effect methods. The rectangle displays three electrochemically accessible reductions assigned as LL based. The singly reduced rectangles are part of an unusual class of mixed-valence complexes where cofacial ligands, in this case porphyrins, comprise the degenerate redox centers. Absorption spectra for the singly reduced rectangle show two intense and narrow absorption bands in the near-infrared (NIR) region; the lower energy band is assigned as an intervalence transition. Time-dependent density functional theory electronic structure calculations support the assignment. Curiously, the transition displays a non-Marcus-type solvent dependence. NIR region electroabsorbance measurements of the singly reduced rectangle reveal a small but readily measurable dipole moment change of 0.56 ± 0.05 eÅ. On the basis of spectroelectrochemical and electroabsorption measurements, the singly reduced rectangle is assigned as a borderline class II/class III mixed-valence species.

Introduction

Among the most useful kinds of systems for understanding fundamental aspects of electron-transfer (ET) reactivity have been mixed-valence compounds, especially those displaying well-resolved intervalence absorption bands. Traditional inorganic mixed-valence complexes (MVCs) usually have the form M^n−bridge−M^{n+1} where M is a transition metal and the bridge consists of an organic linker. Electronic communication between metal ions is typically achieved via through-bridge superexchange processes. This generally means that metal-to-bridge and bridge-to-metal charge transfer states (virtual states) must be accounted for to accurately model and interpret observed spectral features.[1] Metal-based mixed-valence compounds, especially those of second or third row transition metals, often exhibit overly broad intervalence bands because of the existence of multiple nondegenerate d donor orbitals. The nondegeneracy is typically a consequence of both spin−orbit coupling and ligand-field asymmetry. The multiple d orbitals give rise to multiple intervalence transfer (IT) bands that overlap spectrally but differ slightly in energy.[2] Since the accurate extraction of ET-reaction relevant parameters from IT bands depends on the knowledge of the shapes and intensities of individual bands, their overlap complicates their use for this purpose.

We have recently reported on several examples of a new class of MVCs that lack these complexities and complications. The class consists of singly reduced molecular rectangles.[3,4] The rectangles, in their neutral state, have the form $([Re(CO)_3]_2X)_2$-μ,μ'-$[LL]_2$, where LL is one of a pair of redox active ligands (linear dipyridyl or diazine species) arranged cofacially along the long sides of the rectangle and X represents one of two bridging units (μ-alkoxides, μ-thiolates, or 2,2′-bisbenzimidazolates) on the short sides.[5] The Re atoms occupy the four corners of the rectangle. When one of the LL ligands is reduced by an odd number of electrons, the rectangles become MV species where the LL

* To whom correspondence should be addressed. E-mail: jthupp@chem.northwestern.edu.
[†] Northwestern University.
[‡] Georgia Institute of Technology.

(1) Brunschwig, B. S.; Creutz, C.; Sutin, N. *Chem. Soc. Rev.* **2002**, *31*, 168−184.
(2) Demadis, K. D.; Hartshorn, C. M.; Meyer, T. J. *Chem. Rev.* **2001**, *101*, 2655−2685.
(3) Dinolfo, P. H.; Williams, M. E.; Stern, C. L.; Hupp, J. T. *J. Am. Chem. Soc.* **2004**, *126*, 12989−13001.
(4) Dinolfo, P. H.; Hupp, J. T. *J. Am. Chem. Soc.* **2004**, *126*, 16814−16819.

10.1021/ic050834o CCC: $30.25
Published on Web 07/01/2005

ligands are the degenerate redox centers, that is, ligand-centered mixed valency (LCMV) is attained. Within these systems, the four Re atoms serve mainly a structural purpose and do not significantly mediate electronic interaction between ligands. Rather, electronic communication is achieved primarily by direct overlap of the donor and acceptor orbitals, that is, either through-space or close-contact interactions, but not superexchange interactions.[6] Consequently, these compounds comprise relatively rare examples of MVCs that are describable by two-state theories.

The initial studies showed that the magnitude of the electronic interaction characterizing LCMV in these systems can vary by a surprisingly large amount. Encountered were examples spanning the range from nearly class I to fully class III on the Robin−Day classification scale—in other words, from essentially completely valence localized and electronically noninteracting to completely valence delocalized and strongly electronically interacting. The salient structural features were LL/LL approach distance, extent of van der Waals (vdW) or sub-vdW contact, and degree of lateral alignment. Lateral offsets of as little as 2 Å for LL/LL ligand pairs in vdW contact were found to be sufficient to effectively shut off electronic communication (e.g., no observable IT band intensity).[3,4]

With these observations in mind, we reasoned that an LCMV study of a previously synthesized molecular rectangle, a large pyridyl(ethynyl)porphyrin rectangle (**1** shown in Figure 1),[7] could prove interesting. With a ca. 5.7 Å × 24.5 Å rhenium framework, the neutral form of the complex is symmetrically distorted away from a strictly rectangular configuration. In particular, bending of two out of the four ethynyl-pyridines brings the porphyrins into van der Waals contact. The very large contact area (∼100 Å^2), and the presumably small reorganization energy, suggested to us that **1**$^-$ might display class III behavior. At the same time, the observed lateral slippage of the porphyrin planes by ca. 1 Å with respect to each should diminish direct donor-orbital/acceptor-orbital overlap, potentially resulting in class II behavior. As detailed below, we find, in fact, that electronic coupling is substantial but that intervalence excitation apparently does involve a finite amount of porphyrin-to-porphyrin charge transfer. Additionally, we observe distinctly non-Marcus-type solvent effects upon the intervalence band energy maximum.

(5) See also: (a) Benkstein, K. D.; Hupp, J. T.; Stern, C. L. *Angew. Chem., Int. Ed.* **2000**, *39*, 2891−2893. (b) Benkstein, K. D.; Hupp, J. T.; Stern, C. L. *Inorg. Chem.* **1998**, *37*, 5404−5405. (c) Manimaran, B.; Rajendran, T.; Lu, Y.-L.; Lee, G.-H.; Peng, S.-M.; Lu, K.-L. *J. Chem. Soc., Dalton Trans.* **2001**, 515−517. (d) Woessner, S. M.; Helms, J. B.; Shen, Y.; Sullivan, B. P. *Inorg. Chem.* **1998**, *37*, 5406−5407. (e) Kaim, W.; Schwederski, B.; Dogan, A.; Fiedler, J.; Kuehl, C. J.; Stang, P. J. *Inorg. Chem.* **2002**, *41*, 4025−4028. (f) Hartmann, H.; Berger, S.; Winter, R.; Fiedler, J.; Kaim, W. *Inorg. Chem.* **2000**, *39*, 4977−4980.

(6) For examples where through-space interactions dominate (but do not completely define) electronic communication in metal- and organic-based mixed-valence systems, see: (a) Elliott, C. M.; Derr, D. L.; Ferrere, S.; Newton, M. D.; Liu, Y. P. *J. Am. Chem. Soc.* **1996**, *118*, 5221−5228. (b) Sun, D. L.; Rosokha, S. V.; Lindeman, S. V.; Kochi, J. K. *J. Am. Chem. Soc.* **2003**, *125*, 15950−15963.

(7) Benkstein, K. D.; Stern, C. L.; Splan, K. E.; Johnson, R. C.; Walters, K. A.; Vanhelmont, F. W. M.; Hupp, J. T. *Eur. J. Inorg. Chem.* **2002**, *2002*, 2818−2822.

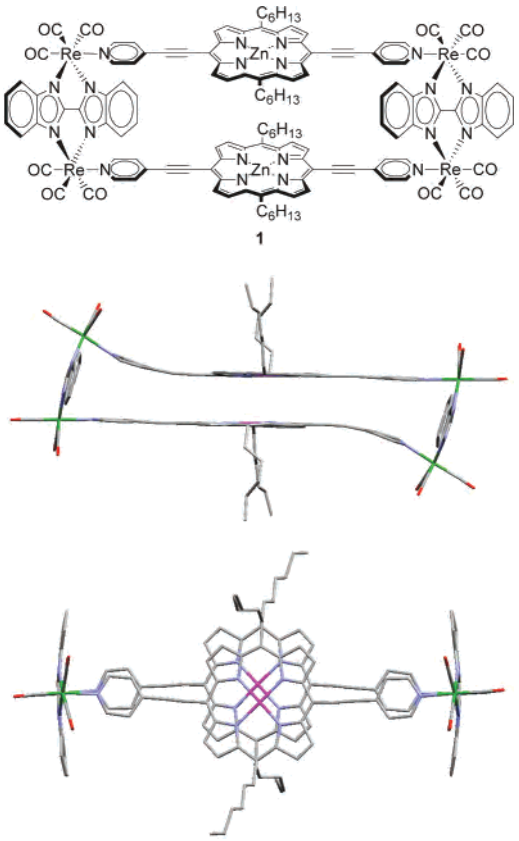

Figure 1. Schematic drawing of **1** and stick model generated from the X-ray crystal structure coordinates (side and top view). Carbon atoms are shown in gray, oxygen in red, nitrogen in blue, zinc in pink, and rhenium in green. Hydrogen atoms were removed for clarity.

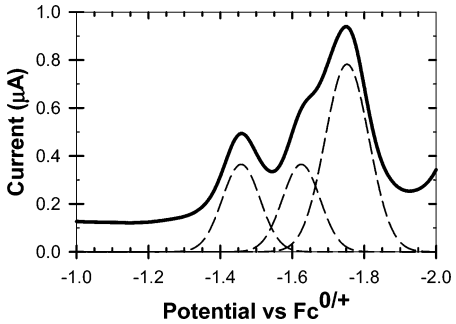

Figure 2. Differential-pulse voltammetry scan for **1** in THF with 0.1 M $TBAPF_6$ as the supporting electrolyte (solid black line). Also shown is the Gaussian deconvolution for each reduction step (dashed black line) after baseline correction.

Results and Discussion

Preliminary Electrochemistry and Spectroelectrochemistry. Figure 2 shows a differential pulse voltammetry scan of **1** in tetrahydrafuran with 0.1 M $TBAPF_6$ as the supporting electrolyte. Also shown is a Gaussian deconvolution. From the deconvolution, the formal reduction potentials vs ferrocene/ferrocinium as an internal reference are $E_f^{0/-} = -1.45$ V, $E_f^{-/2-} = -1.64$ V, and $E_f^{2-/4-} = -1.75$ V. The values obtained differ slightly from those previously reported by us,[7] probably because of an error in converting reference potentials in the earlier study. Most important here, however, are the potential *differences* because they provide measures of mixed-valence-state stability with respect to neighboring

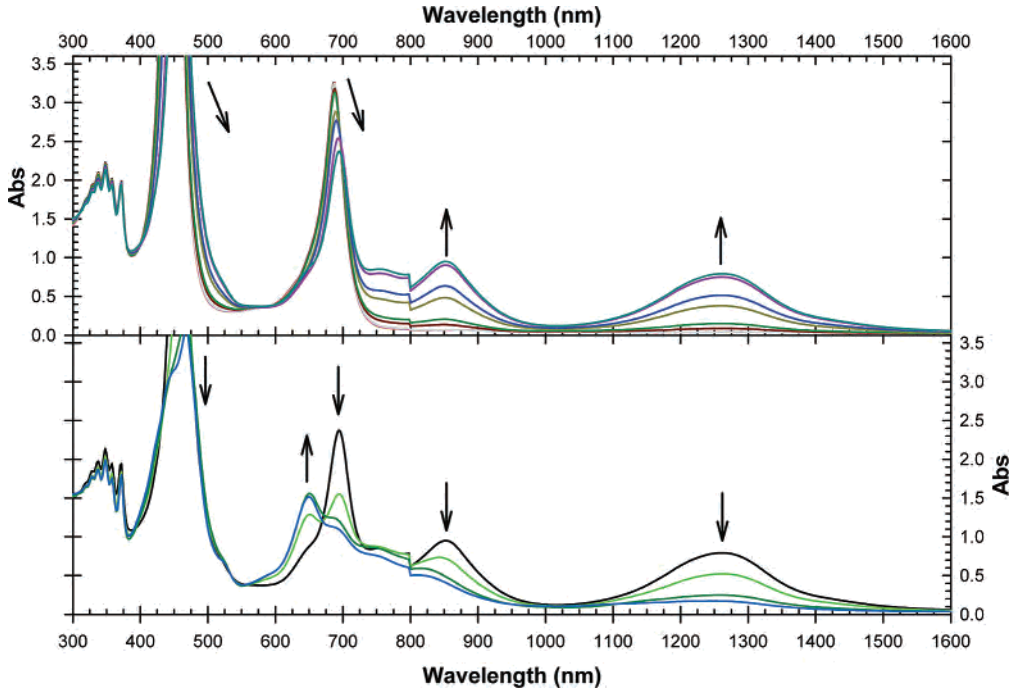

Figure 3. UV−vis−NIR absorption scans of **1** obtained in THF, during a spectroelectrochemical measurement with 0.1 M $TBAPF_6$ as the supporting electrolyte. The top panel shows the reduction from the neutral to 1− state, and the bottom panel shows the reduction from the 1− to 2− state. The absorbance irregularity at 800 nm is due to the change in instrument detector.

redox states. The 190 mV difference between the first two reduction potentials of **1** corresponds to a greater than 95% preference for the singly reduced mixed-valence form. A second mixed-valence ion, the triply reduced version of **1**, clearly is much less well stabilized with respect to redox disproportionation. The exact amount is difficult to determine via voltammetry alone because peaks for the 2−/3− and 3−/4− couples are not resolved. A lower-limit estimate is the statistical limit, that is, 50% as $\mathbf{1}^{3-}$ and 25% each as $\mathbf{1}^{2-}$ and $\mathbf{1}^{4-}$.

One explanation for the stability differences is geometric differences. In the collapsed conformation, addition of a second electron would (in the valence localized limit) engender significant porphyrin/porphyrin electrostatic repulsion, thereby energetically inhibiting the process or, equivalently, displacing the second reduction potential to a significantly more negative value. On the other hand, assuming the repulsion leads to an open-cavity conformation for $\mathbf{1}^{2-}$, progressive addition of the third and fourth electrons should occur with little electrostatic penalty and, therefore, little difference between $E_f^{2-/3-}$ and $E_f^{3-/4-}$.[8] (Similarly, interligand electrostatics should contribute in only a minor way to the difference in potential between the 1−/2− and 2−/3− couples—the observed difference instead reflecting the cost of placing an additional electron into an already partially occupied orbital.)

Assignment of the observed reductions as porphyrin centered is supported by UV−vis−near-infrared (NIR) spectroelectrochemical (SEC) measurements. Figure 3 shows a series of UV−vis−NIR absorption spectra for **1** during a typical SEC measurement in THF. The top panel (a) shows the reduction from the neutral to 1− state. Observed in addition to red shifts and intensity losses in the Soret and Q-band regions is the appearance of two new absorption bands in the NIR region, specifically at 860 and 1250 nm. Notably the two new bands disappear upon conversion to the 2− state (panel b). Further reduction to the 4− state is accompanied by broadening of the Soret and Q-bands and the appearance of several new bands between 900 and 1100 nm (not shown). A more careful evaluation of the spectra reveals that more than one additional species appears during the course of the second reduction, as expected, of course, if the 3− form is present to a significant extent at the intermediate stages of the SEC reduction. The new peak at 640 nm (bottom panel) continues to grow as the assembly is reduced to the 3− and 4− states.

Consistent with the redox assignments, the high-energy bands (<400 nm) associated with the BiBzIm bridging ligands are largely unaffected by the various reductions. A similar pattern is observed for **1** in CH_2Cl_2 as solvent, except that all of the porphyrin-based absorption bands are blue shifted relative to those obtained in THF.

Returning to the NIR part of the spectrum, the bands present in the 1− state, and not observed in the 0, 2−, 3−, and 4− states, are clearly electronic in nature. It is tempting to assign both as IT bands. As implied above, spectrally resolved multiple IT bands have occasionally been reported

(8) An energetic and geometric subtlety may exist here. Recall that van der Waals forces (responsible for assembly collapse) are exceptionally short-range forces. If they are counterbalanced by an electrostatic interaction sufficient enough to separate the porphyrin ligands slightly, significant further separation should occur, with minimal additional loss of favorable van der Waals interactions, because of the geometric stabilization (covalent bond stabilization) obtainable by restraightening the two bent ethynyl pyridine moieties. The fully expanded conformation then leads to smaller-than-otherwise-expected ligand/ligand electrostatic repulsions (and charge-state differences in repulsion) for the 2−, 3−, and 4− assemblies.

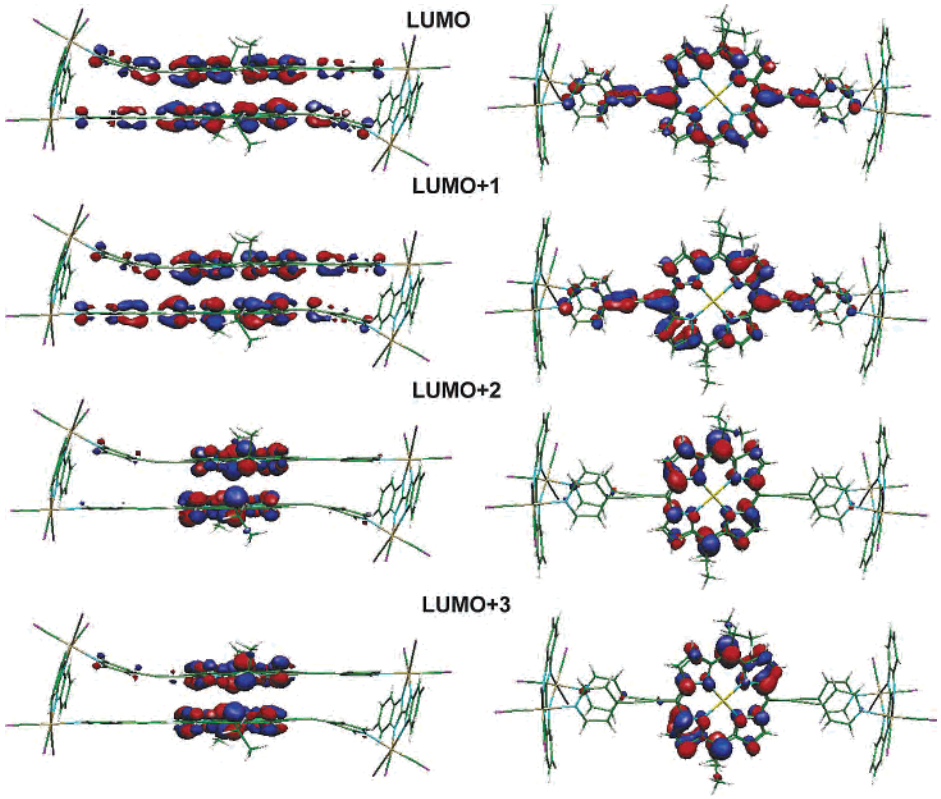

Figure 4. Contour plots of the B3LYP/LANL2DZ derived LUMO through LUMO+3 molecular orbitals of **1**, viewed from side (left) and top (right).

for traditional inorganic mixed-valence compounds featuring metals having large spin−orbit coupling constants.[9] Electronic structure calculations discussed in the following section indicate, however, that only the lower energy band is associated with intervalence excitation.

Electronic Structure Calculations

Time-dependent density functional theory (TD-DFT) calculations were performed to provide some insight into the intervalence spectroscopy. (Similar trends were obtained from semiempirical (restricted open-shell Hartree−Fock) Zerner's intermediate neglect of differential overlap (ZINDO) level calculations.)[10] The starting point was the neutral version of **1**, fixed at the crystallographically determined geometry. Single-point DFT calculations of the full system revealed that the frontier orbitals are entirely localized on the porphyrin segments; see Figure 4. The calculated energy difference between the LUMO and LUMO+1 orbitals is ~660 cm^{-1}; this leads to a Koopman's theorem (KT) estimate of 330 cm^{-1} for H_{ab}, the electronic coupling matrix element for ligand-to-ligand charge transfer in the corresponding anionic assembly. Repeating the calculation at the same geometry, while omitting the rhenium centers and the ancillary ligands, yields a KT estimate for H_{ab} of 335 cm^{-1}. The similarity underscores the importance of direct donor-orbital/acceptor-orbital overlap and the *un*importance of indirect coupling through the tetrarhenium framework.

In view of these findings, subsequent calculations were carried out without the rhenium atoms and nonporphyrinic ligands. The TD-DFT results obtained for the simplified version of the singly reduced dimer, again using the X-ray coordinates of the neutral assembly, indicate that the first optical band at 1200 cm^{-1} is because of an electronic transition that mainly involves two molecular orbitals, closely resembling the LUMO and LUMO+1 orbitals of Figure 4. Therefore, this band is assigned to a porphyrin−porphyrin charge-transfer transition. Even though the TD-DFT H_{ab} estimate of 600 cm^{-1} is larger by a factor of 2 than the KT estimate, the calculated value is still much smaller than that derived from optical data (vide infra). We assign this discrepancy as most likely due to geometric differences between the neutral vs singly reduced versions of **1**.[11] In the neutral geometry (used for the KT and TD-DFT estimates), the porphyrin planes are laterally offset and present relatively poor orbital overlap. The resonance interaction in the singly reduced form would provide an energetic incentive for decreasing the offset and increasing the donor-orbital/acceptor-orbital overlap, thereby maximizing the electronic coupling; such a behavior has been suggested previously for benzene dimers.[12]

When carrying out the TD-DFT calculations for a situation where the lateral offset between porphyrin planes is set to

(9) Kober, E. M.; Goldsby, K. A.; Narayana, D. N. S.; Meyer, T. J. *J. Am. Chem. Soc.* **1983**, *105*, 4303−4309.
(10) Zerner, M. C.; Loew, G. H.; Kirchner, R. F.; Mueller-Westerhoff, U. T. *J. Am. Chem. Soc.* **1980**, *102*, 589−599.
(11) Geometric differences also likely account for the absence of observable intervalence band intensity in the triply reduced form of **1**. As discussed above, an open-cavity geometry (and therefore reduced orbital overlap and intervalence intensity) would be expected based on porphyrin-anion/porphyrin-anion electrostatic repulsion.
(12) Inokuchi, Y.; Naitoh, Y.; Ohashi, K.; Saitow, K.; Yoshihara, K.; Nishi, N. *Chem. Phys. Lett.* **1997**, *269*, 298−304.

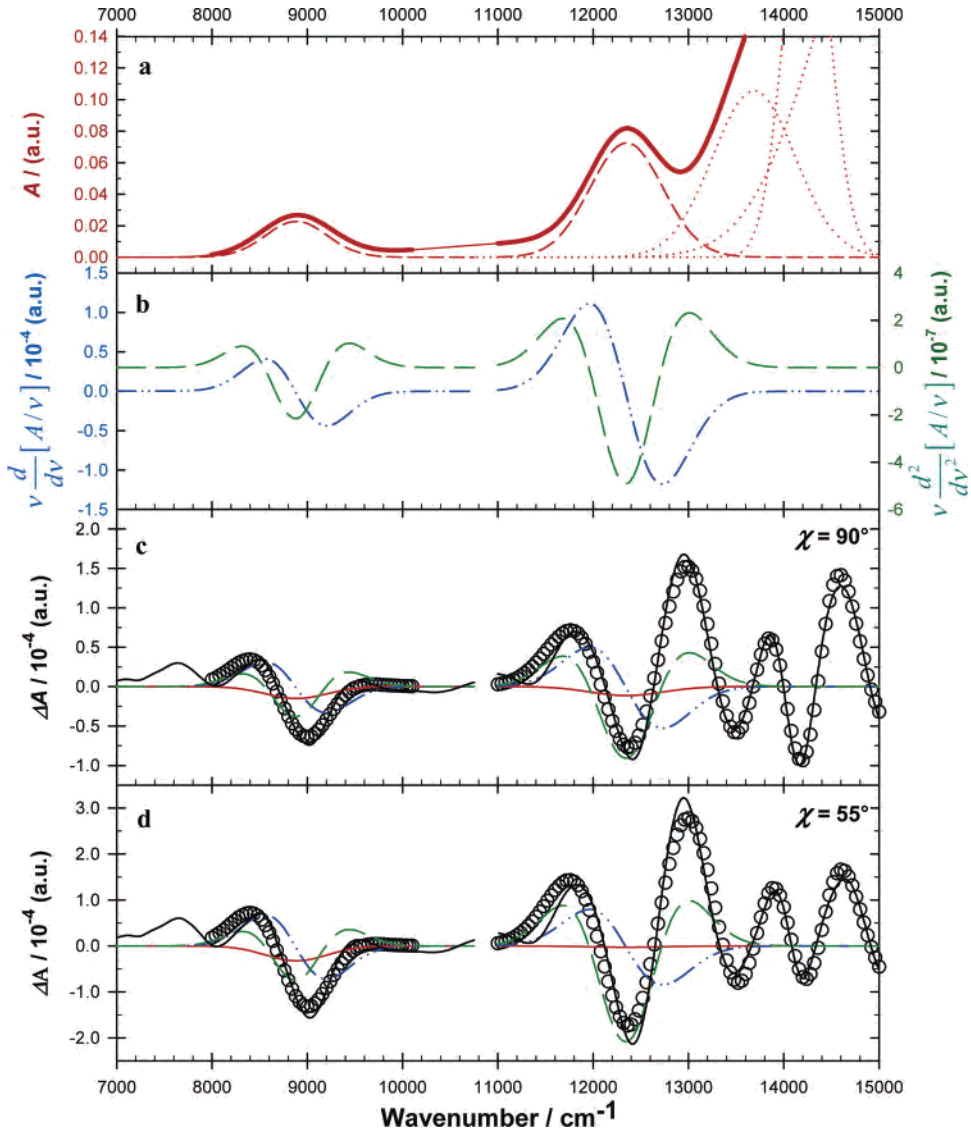

Figure 5. Stark spectra and Liptay analysis (see Experimental Section) spectra for $\mathbf{1}^-$. Panel a: unperturbed absorption spectrum at 77 K in 4:1 MeTHF/butyronitrile (solid red line). Dashed and dotted lines are Gaussian deconvolutions. Panel b: frequency-weighted first and second derivatives of absorption spectrum (dashed−dotted blue line and dashed green line, respectively). Panels c and d: measured (solid black lines) and fit (open circles), Stark signals at $\chi = 90°$ and 55°, respectively. Independent fitting was done in two portions of the spectrum (indicated by bold red lines in the top panel). Included with the fits are the contributions from the zeroth, (red) and the first and second derivatives (dashed−dotted blue line and dashed green line, respectively) of the frequency-weighted absorption spectrum.

zero, we obtain a much better agreement between the theoretical and experimental results. The TD-DFT calculations performed for a 3.5 Å separation between the porphyrins (i.e., in van der Waals contact) reveal the following:

(a) The lowest energy transition is a forbidden transition localized on one porphyrin.

(b) The next transition is an allowed porphyrin-to-porphyrin charge-transfer, that is, intervalence transition. Its energy corresponds to 6400 cm^{-1} (1560 nm) with an oscillator strength of 0.097. The corresponding transition dipole moment is oriented normal to the porphyrin planes, as required for a porphyrin−porphyrin charge-transfer transition. The absorption band seen experimentally at 1250 nm can be identified with this transition. It is important to note that the energy and intensity of this transition are dependent on the donor/acceptor separation distance and the extent of deviation from a cofacial configuration. Separating the porphyrins or increasing the offset between porphyrin planes leads, as expected, to a precipitous drop in the transition intensity and, consequently, in the estimate for H_{ab}.

(c) A second intervalence transition occurs at $E = 9200$ cm^{-1} (1090 nm). The calculated intensity, however, is zero as a consequence of zero net orbital overlap. It is conceivable that this transition could acquire some intensity via vibronic mixing. In the absence of such an effect, though, the band observed experimentally at 860 nm cannot be assigned to this transition.

(d) A porphyrin-localized transition of reasonable intensity (oscillator strength = 0.20) is found at 10 300 cm^{-1} (970 nm). On the basis of its intensity, the experimentally observed band at 860 nm is tentatively assigned to this transition rather than to a second intervalence transition.

Electroabsorption Spectroscopy and Mixed-Valence Analysis. Electroabsorption spectroscopy measures the elec-

tric field induced change in molar absorptivity for a randomly orientated and immobilized sample. The change in absorption, the Stark spectrum, can be related to changes in molecular polarizability and dipole moment associated with optical excitation. Notably, the change in dipole moment, $\Delta\mu_{12}$, can be related to the adiabatic charge-transfer distance, R_{12}, via eq 1

$$\Delta\mu_{12} = eR_{12} \tag{1}$$

where e is the unit electronic charge.

Mixed-valent rectangular samples for Stark analysis were generated by chemical reduction using 5% Na(Hg) in the presence of excess 15-crown-5, a sodium ion complexing agent. (This method proved to be superior to electrochemical methods for generating the more concentrated solutions required for Stark measurements.)

Figure 5 (panel a) shows the unperturbed absorption spectrum at 77 K along with the deconvoluted bands associated with the intervalence transition (T_1) and the transition near 860 nm (T_2) (dashed red lines) and Q-bands (dotted red lines). Both low-energy bands are blue shifted (T_1 by ca. 800 cm^{-1} and T_2 by ca. 200 cm^{-1}) and narrowed relative to the bands measured at room temperature. Panel b shows the frequency-weighted first and second derivatives of the experimental absorption spectrum. The measured Stark responses (ΔA) at $\chi = 90$ and 55° are shown as solid black lines in panels c and d, respectively. Fits are shown as open circles. Also shown are the relative contributions to the fits from zeroth-, first-, and second-derivative components. The wavelength ranges over which the Stark signals were fit are indicated by the bold portions of the red line in panel a. Qualitatively, it can be seen that the second-derivative components (indicative of charge transfer) are strong contributors to the intervalence Stark spectra.

For T_1, a quantitative Liptay analysis (see Experimental Section for details) using measurements made at both angles revealed an absolute dipole moment change ($|\Delta\mu|$) of 0.56 ± 0.05 e Å and polarizability changes of $\mathrm{Tr}(\Delta\alpha) = 150 \pm 9$ $Å^3$ and $\Delta\alpha = 180 \pm 14$ $Å^3$. The analysis showed, as expected, that the transition dipole moment and $\Delta\mu$ vectors are collinear. The higher energy band (T_2), while displaying a well-resolved peak, overlaps to a degree with the tail of the lowest energy Q-band. Consequently, only two-thirds of the T_2 Stark spectrum (i.e., the low-energy portion) was initially fit. The quantities obtained were $|\Delta\mu| = 0.65 \pm 0.02$ eÅ, $\mathrm{Tr}(\Delta\alpha) = 49 \pm 3$ $Å^3$, and $\Delta\alpha = 63 \pm 8$ $Å^3$. (The uncertainties reported are fitting uncertainties based on four independent measurements, not overall measurement uncertainties.) Not surprisingly, slightly better fits statistically were obtained for T_2 by fitting a series of Gaussian components spanning the T_2 + Q-band region. The values returned by the fit, however, were only marginally different. Additionally, the analyses showed for both transitions that the transition dipole moment and $\Delta\mu$ vectors are collinear.

With values for $|\Delta\mu|$ ($= eR_{12}$) in hand, Hush's treatment (beginning with eq 2) was used to extract estimates of the initial-state/final-state electronic coupling energy (H_{ab}) from the experimental intervalence absorption spectra. In eq 2,

$$H_{ab} = \frac{0.0206}{R_{ab}}\sqrt{\nu_{max}\epsilon_{max}\Delta\nu_{1/2}} \tag{2}$$

R_{ab} is the diabatic electron-transfer distance and ν_{max}, ϵ_{max}, and $\Delta\nu_{1/2}$ are the absorption peak energy, molar absorptivity, and bandwidth, respectively.[13,14] To obtain R_{ab} from Stark-determined R_{12} values, we employed the generalized Mulliken−Hush analysis, as prescribed by Cave and Newton and summarized in eq 3[15,16]

$$R_{ab}/e = \sqrt{(R_{12}/e)^2 + 4(\mu_{12})^2} \tag{3}$$

where R_{12} is the value obtained from eq 1 and μ_{12} is the transition dipole moment in eÅ, as estimated via eq 4 from the intervalence absorption parameters.

$$\mu_{12} = \sqrt{\frac{\epsilon_{max}\Delta\nu_{1/2}}{\nu_{max}}} \tag{4}$$

The values obtained for μ_{12}, R_{ab}, and H_{ab} for T_1 are 1.37 eÅ, 2.8 Å, and 3900 cm^{-1}, respectively, using data for THF as the solvent. The experimental estimate of $H_{ab} = 3900$ cm^{-1} is bracketed by the TD-DFT values[17] of 4600 and 3200 cm^{-1} derived for 3.2 and 3.5 Å porphyrin−porphyrin separation, respectively. The diabatic distance corresponds to the electron-transfer distance under hypothetical conditions of zero electronic coupling. The value obtained here is in fair agreement with the ~3.4 Å porphyrin−porphyrin separation distance for a cofacial van der Waals contact geometry; we note that for strongly interacting systems, the experimentally determined R_{ab} values are often slightly smaller than geometric donor/acceptor separation distances.[3]

Qualitatively, the large value obtained for H_{ab} is indicative of extensive ground-state valence delocalization or, equivalently, transfer of only a small fraction of an electronic charge upon intervalence excitation. From eq 5, the fraction of

$$\Delta qR_{ab} = eR_{12} \tag{5}$$

charge transferred, Δq, is ~0.2. Alternatively, Hush's delocalization parameter, α', taken as H_{ab}/ν_{max}, is 0.49, that is, the amount of charge already transferred from donor to acceptor in the electronic ground state. In the framework of the two-state limit where the fraction of charge transferred

$$\Delta q = 1 - 2\alpha' \tag{6}$$

(13) Hush, N. S. *Prog. Inorg. Chem.* **1967**, *8*, 391−444.
(14) Hush, N. S. *Coord. Chem. Rev.* **1985**, *64*, 135−157.
(15) Cave, R. J.; Newton, M. D. *Chem. Phys. Lett.* **1996**, *249*, 15−19.
(16) Cave, R. J.; Newton, M. D. *J. Chem. Phys.* **1997**, *106*, 9213−9226.
(17) We note that TD-DFT calculations should be used with care, since it is known that, because of inherent problems in the applied standard exchange-correlation functionals, TD-DFT fails to describe adequately the charge-transfer transitions in weakly electronic coupled systems. See for instance: (a) Grimme, S.; Parac, M. *ChemPhysChem* **2003**, *4*, 292−295. (b) Dreuw, A.; Weisman, J. L.; Head-Gordon, M. *J. Chem. Phys.* **2003**, *119*, 2943−2946.

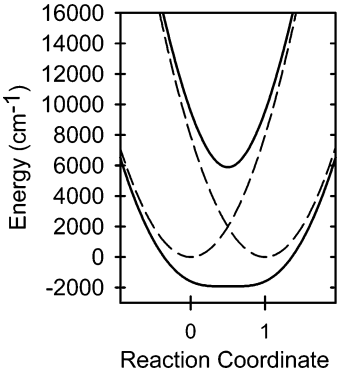

Figure 6. Calculated potential energy surfaces for $\mathbf{1}^-$ based on the two-state Hush model. Adiabatic surfaces are shown as solid lines and diabatic surfaces as dashed lines. The values, taken from measurements in THF, were $\lambda = \nu_{max} = 7940\ cm^{-1}$ and $H_{ab} = 3900\ cm^{-1}$.

upon optical excitation (or thermal electron exchange) is negligible (0.02) and the system can then be viewed as essentially fully delocalized.

Shown in Figure 6 are the adiabatic and diabatic surfaces for the ground state and intervalence excited state of $\mathbf{1}^-$. The surfaces were obtained from the Hush theory, as outlined by Brunschwig and Sutin in their generalized description of two-state systems featuring parabolic diabatic surfaces.[1] Consistent with the near equivalence of λ ($=\nu_{max} = 7940\ cm^{-1}$) and $2H_{ab}$ ($7800\ cm^{-1}$), a nearly barrierless ground-state surface, the characteristic of a borderline class II/class III system is obtained.

Solvent Dependence

Intervalence band energies for class II mixed-valence complexes, when evaluated in multiple solvents, often vary with the difference of the reciprocals of the optical and static dielectric constants of the solvent. The origin of the correlation is in Marcus-type solvent polarization contributions to the reorganization energy. Intervalence band energies for strongly class III systems ($2H_{ab} \gg \lambda$) often are insensitive to solvent. For less strongly coupled class III systems ($2H_{ab} > \lambda$) and borderline class II−class III systems ($2H_{ab} \approx \lambda$), modest changes in band energy with changes in solvent have been seen; however, the energy changes often correlate with properties other than dielectric parameters.[18,19] Figure 7, a comparison of the SEC-determined T_1 absorption spectrum in THF vs CH_2Cl_2, shows that a solvent dependence exists for intervalence excitation of the porphyrin assembly. In contrast to expectations from Marcus and related non-equilibrium solvent polarization theories, however, the absorption energy maximum for T_1 is higher in CH_2Cl_2 than in THF. Furthermore, the band in THF is asymmetric, with diminished intensity on the low energy side, whereas in CH_2Cl_2 it is nearly Gaussian. (The bandwidths at half-height are nearly identical, $1180\ cm^{-1}$ in CH_2Cl_2 and $1240\ cm^{-1}$ in THF.) The asymmetry observed in THF, in agreement with the trend shown by bands intensities, is a signature of a larger electronic coupling in THF vs CH_2Cl_2.[20]

(18) Creutz, C.; Chou, M. H. *Inorg. Chem.* **1987**, *26*, 2995−3000.
(19) Nelsen, S. F.; Konradsson, A. E.; Telo, J. P. *J. Am. Chem. Soc.* **2005**, *127*, 920−925.

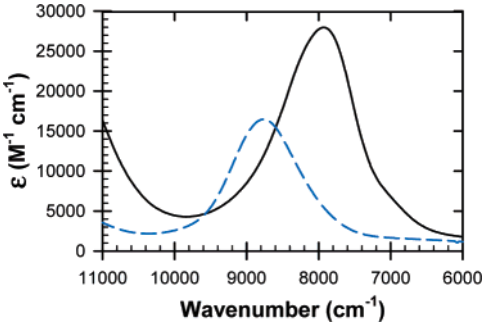

Figure 7. Intervalence absorption band of $\mathbf{1}^-$, determined spectroelectrochemically in THF (solid black line) and CH_2Cl_2 (dashed blue line), with 0.1 M $TBAPF_6$.

Additional measurements were made in dimethylformamide, pyridine, and a 4:1 mixture of MeTHF and butyronitrile. In these solvents, the mixed-valence species was generated via chemical reduction, rather than electrochemically, by using sodium amalgam in the presence of 15-crown-5. (Unfortunately, MVC insolubility or solvent reduction prevented measurements in several other candidate solvents.) Notably, application of the chemical approach to **1** in THF yielded T_1 and T_2 energies differing only slightly from the SEC-determined values. The results are summarized in Table 1. The intervalence band energies appear to be progressively red shifting as the solvent's Lewis basicity increases.[21] The behavior parallels that generally seen for Soret and Q-bands in Zn(II) porphyrins where the shifts are clearly associated with Zn(II) axial ligation. For the IT band, the apparent correlation might simply be indicative of mixing of the intervalence excited state with higher-energy excited states.

Potential Alternative Analysis

The Mulliken−Hush analysis employed above assumes the separability of nuclear and electronic motion. An alternative approach—one that becomes increasingly attractive as the classII/class III boundary is approached—is to relax the separability requirement and employ a vibronic coupling treatment.[22] That a vibronic coupling approach may well be of added value here is suggested by the observed intervalence line widths. These are only about half the width predicted by the Hush two-state model in the classical limit;[13] much narrower line widths can be obtained from vibronic coupling models.

Treynor and Boxer have recently presented a critical discussion of such treatments and considered how they can

(20) Ligation of the Zn(II) centers by THF (as opposed to very weak ligation by methylene chloride) should increase the overall electron density on the porphyrin ligands, potentially accounting for the increase in electronic coupling.
(21) Unfortunately, baseline problems (probably due to the slow decomposition of the doubly reduced assembly) were encountered with the chemical reduction method. We suspect that these account for the slight difference between energies recorded following chemical vs electrochemical reduction. Most affected by baseline problems were measurements made in dimethylformamide as solvent, making these the least reliable entries in the table. The true energies in DMF are likely slightly smaller than those reported.
(22) See, for example: (a) Piepho, S. B. *J. Am. Chem. Soc.* **1988**, *110*, 6319−6326. (b) Piepho, S. B.; Krausz, E. R.; Schatz, P. N. *J. Am. Chem. Soc.* **1978**, *100*, 2996−3005. (c) Coropceanu, V.; Malagoli, M.; Andre, J. M.; Bredas, J. L. *J. Am. Chem. Soc.* **2002**, *124*, 10519−10530.

Table 1. Near-Infrared Band Absorption Data

T_1			T_2	conditions	
ν_{max} (cm^{-1})	ϵ (M^{-1} cm^{-1})	$\Delta\nu^{1/2}$ (cm^{-1})	ν_{max} (cm^{-1})	solvent	technique/counter ion
8760	16500	1180	12440	CH_2Cl_2	SEC/TBA
7940	28000	1260	11740	THF	SEC/TBA
8100	NA	NA	11900	THF	chemical/Na^+[15-C-5]
8090	NA	NA	12220	MeTHF/PrCN (4:1)	chemical/Na^+[15-C-5]
8300	NA	NA	12240	DMF	chemical/Na^+[15-C-5]
7920	NA	NA	11650	pyridine	chemical/Na^+[15-C-5]

be implemented in the context of electroabsorbance measurements, specifically for mixed-valence species.[23] One finding is that first-derivative components of Stark spectra can contain significant contributions from dipole moment changes, in addition to the expected polarizability information.[24] Another is that the apparent dipole moment changes extracted from a Liptay analysis can differ from the true changes. In several, but not all, of the test cases modeled, the differences were small. One diagnostic of analysis failure was found to be a deviation of the measured Stark signal magnitude from the expected dependence on the square of the applied field, although in some instances where failure occurred reasonable adherence to field-squared behavior was still found. In any case, we observed the expected field-squared dependence in our measurements (which spanned a factor of 8 in field strength).

Another diagnostic demonstrates substantial departures of the Liptay fit (i.e., a frequency-weighted sum of zeroth-, first-, and second-derivative absorbance spectral contributions) from the experimental spectrum, although again not every poorly behaved case showed such departures. Although it may be inappropriate to generalize, the one example presented of poor behavior (in terms of fidelity of the Liptay-determined value of the dipole moment change) coupled with an excellent empirical fit of the Stark spectrum was characterized by a dominant first-derivative contribution to the spectrum. In contrast, we have not observed substantial departures from the empirical Liptay fits, nor is the spectrum for $\mathbf{1}^-$ dominated by a first-derivative contribution. Together with the observed normal field-dependence, these findings suggest, but do not prove, that the analysis used has returned reasonably accurate estimates for R_{12}.

A criterion for delocalization that is expected to hold regardless of whether vibronic coupling is important is $\mu_{12} \geq eR_{ab}/(2\sqrt{2})$.[23] If vibronic coupling is significant, however, the Mulliken−Hush analysis (which assumes separability) should not be used to estimate R_{ab}, leaving this as an undetermined quantity. An obvious choice, though, is the porphyrin−porphyrin center-to-center distance—about 3.4 Å for a collapsed geometry. On this basis, $eR_{ab}/(2\sqrt{2})$ is 1.2 eÅ. For comparison, μ_{12} for $\mathbf{1}^-$ is 1.37 eÅ (THF) or 0.97 eÅ (CH_2Cl_2). These results suggest a class III or perhaps borderline class III/class II description, the greatest uncertainty in the analysis being the value of R_{ab}. Additional experimental molecular structural studies and a quantitative vibronic analysis—both beyond the scope of this report—could prove to be informative.

Conclusions

Intervalence absorption due to ligand-centered mixed valency is readily observable for **1**, its singly reduced form. Electronic communication occurs by direct donor-orbital/acceptor-orbital overlap, rather than superexchange coupling, and is likely facilitated by a collapsed geometry that places the cofacial porphyrins in vdW contact. The resulting strong coupling gives rise to two intense low-energy transitions, one of which is found by electronic structure calculations to be an intervalence transition. The ground-state mixed-valence species appears to be a borderline completely delocalized system. Stark effect spectroscopy confirms both the residual charge-transfer nature of the low energy absorption band and the large, but not quite complete, degree of delocalization. Regarding the solvent effects upon intervalence, the intervalence spectrum is uncorrelated with the solvent parameters of Marcus theory and instead appears to be associated with specific effects involving axial ligation of the Zn(II) porphyrins. The triply reduced assembly also comprises a ligand-

(23) Treynor, T. P.; Boxer, S. G. *J. Phys. Chem. A* **2004,** *108*, 1764−1778.

(24) The non-Liptay first-derivative contribution can appear regardless of whether vibronic coupling is important. Its origin is in the double-welled ground potential energy surface that characterizes symmetrical class II mixed-valence species. In the presence of a tiny applied field, essentially equal numbers of MV molecules will be oriented with dipole moments parallel to the field vs antiparallel to it. In the presence of a large field, one orientation will be significantly energetically stabilized and the other will be destabilized. Consequently, the intervalence band for one will be slightly blue-shifted, and the intervalence band for the other red-shifted. This is the origin of the standard Stark spectral broadening effect that appears as a second-derivative contribution to the electroabsorbance spectrum. A large field, however, can shift a significant portion of the population of one orientation (the energetically destabilized one) to the other orientation (the energetically stabilized one), with the shift being accomplished simply by intramolecular electron transfer. The field, therefore, generates more of the blue-shifted form. The blue shift appears in the difference spectrum (Stark spectrum) as a first-derivative contribution. The effect ought to show up, to a degree, whenever a completely symmetrical double-welled system is examined. In a low dielectric matrix, such as a glass used for Stark measurements, however, the mixed-valence species and its counterion will tend to pair. Ion pairing is well-known to introduce an energetic asymmetry in mixed-valence molecules because the ion preferentially interacts with the more highly charged half of the molecule. In extreme cases, the asymmetry can reach a few hundred millielectronvolts. (See, for example: Blackbourn, R. L.; Dong, Y.; Lyon, L. A.; Hupp, J. T. *Inorg. Chem.* **1994**, *33*, 4446−4452.) The non-Liptay blue-shift effect, therefore, will become important only when the external field is sufficient to offset the pairing-induced redox asymmetry. The system examined here may well be such a case since the charge of the mixed-valence assembly is low and the cation and anion sizes are relatively large. On the other hand, the effects of the external field are also low: about 24 meV for the conditions in Figure 6, if the molecule is perfectly aligned and a 3.4 Å charge-transfer distance is assumed. Notably, the spectrum measured at a quarter of this field strength yields the same values (within a few percent, i.e., smaller than the fitting uncertainties) for dipole moment changes and polarizability changes. Nevertheless, the values obtained here for polarizability changes probably should not be taken too seriously.

centered mixed-valence species but lacks an observable intervalence transition. Electrochemical data suggest that the assembly adopts an open-cavity geometry in the 2−, 3−, and 4− states. The resulting physical separation of the porphyrinic redox centers would essentially eliminate direct orbital overlap and preclude significant intervalence intensity.

Experimental Section

Materials. 1 was available from a previous study.[7] Butryonitrile, 2-methyltetrahydrofuran (MeTHF), and pyridine were purchase from Aldrich and stored over 4 Å molecular sieves. Tetrahydrofuran (THF), methylene chloride, and dimethylformamide (DMF) were purified using a two-column solid-state purification system (Glass-contour System, Joerg Meyer, Irvine, CA). Na(Hg) (5%) and 15-crown-5 were purchased from Aldrich and used with any further purification.

Electrochemistry. All of the cyclic voltammetric experiments were performed and analyzed using a CHI900 (CH Instruments, Austin, TX) potentiostat. Electrolyte solutions (0.1 M tetrabutylammonium hexafluorophosphate ($TBAPF_6$) (>99%, Fluka)) were prepared with anhydrous solvents and nitrogen degassed before use. A Pt wire was used as the counter electrode, and a 2 mm diameter Au macro disk electrode was used as the working electrode. A silver wire was used as a pseudo reference electrode, with ferrocene (Aldrich, purified by sublimation) added as an internal reference at the end of each experiment. All of the experiments were run under an N_2 atmosphere.

Spectroelectrochemistry. UV−vis−NIR SEC experiments were performed with a previously described cell[3] using a Varian CARY 5000 spectrometer and a Princeton Applied Research model 273 potentiostat.

Chemical Reductions. All of the samples were prepared under a dry nitrogen atmosphere (benchtop glovebag). Typically, 1−2 mg of **1** was added to 2 mL of anhydrous, nitrogen degassed solvent, with 1−2 drops of 15-crown-5, in a 1 mm quartz cuvette with a Teflon screw-top. The samples were then reduced with 5% Na-(Hg), while monitoring their UV−vis−NIR absorbance.

Electronic Structure Calculations. All of the DFT and TD-DFT calculations were performed with the Gaussian 03 program[25] at the B3LYP[26−28] level using a LANL2DZ basis set and corresponding effective core pseudopotential. The LL ligands were set planar in dimer-model calculations.

Electroabsorption Spectroscopy (Stark Spectroscopy). A sample of **1** was reduced in a 4:1 MeTHF−butyronitrile solution, using the same techniques as describe above, except the concentration was approximately 5−10 times higher. Stark absorption measurements were conducted in a fashion similar to previous reports[4] but with one modification: in addition to the photovoltaic HgCdTe detector (Judson Technologies) employed for near-infrared regions, a Si PIN Photodiode detector (Thorlabs) was used for visible regions.

Stark Absorption Analysis. Analysis of the data was performed using the Liptay method[29,30] as described in detail elsewhere[31] and only briefly summarized here. Each Stark spectrum was fit to a linear combination of the zeroth, first, and second derivatives of the low-temperature absorption spectrum $A(\upsilon)$ In eq 7, $\Delta A(\upsilon)$ is

$$\Delta A(\upsilon) = \left\{ A_\chi A(\upsilon) + \frac{B_\chi \upsilon}{15hc} \frac{\mathrm{d}[A(\upsilon)/\upsilon]}{\mathrm{d}\upsilon} + \frac{C_\chi \upsilon}{30h^2c^2} \frac{\mathrm{d}^2[A(\upsilon)/\upsilon]}{\mathrm{d}\upsilon^2} \right\} \mathbf{F}_{\mathrm{int}}{}^2 \tag{7}$$

the frequency-dependent absorption change resulting from electric field modulation, h is Planck's constant, c is the speed of light in a vacuum, and υ is the frequency of the absorbed light. The $\mathbf{F}_{\mathrm{int}}$ value is the internal electric field experienced by the chromophore and can be written as

$$\mathbf{F}_{\mathrm{int}} = f\mathbf{F}_{\mathrm{ext}} \tag{8}$$

where $\mathbf{F}_{\mathrm{ext}}$ is the externally applied electric field and f is the local-field correction. The value, $f = 1.3$, typically used for organic solvents,[32] was assumed for all of the calculations. It should be noted, however, that uncertainties of perhaps 20% exist for f. The coefficients A_χ, B_χ, and C_χ provide information about electric-field-induced changes in the transition dipole moment and about excited-state/ground-state polarizability and dipole moment differences, respectively. The molecular parameters are determined as follows

$$A_\chi = \frac{\langle \alpha_{\mathbf{m}} \rangle}{3} + \frac{1}{30}(3\cos^2\chi - 1)[3\langle \beta_{\mathbf{m}} \rangle - 2\langle \alpha_{\mathbf{m}} \rangle] \tag{9}$$

$$B_\chi = \frac{5}{2}\mathrm{Tr}\Delta\alpha + (3\cos^2\chi - 1)\left(\frac{3}{2}\hat{\mathbf{g}}\cdot\Delta\alpha\cdot\hat{\mathbf{g}} - \frac{1}{2}\mathrm{Tr}\Delta\alpha\right) \tag{10}$$

$$C_\chi = |\Delta\mu_\upsilon|^2[5 + (3\cos^2\xi - 1)(3\cos^2\chi - 1)] \tag{11}$$

In these equations, $\langle \alpha_{\mathrm{m}} \rangle$ and $\langle \beta_{\mathrm{m}} \rangle$ are the scalar portions of the transition moment polarizability and hyperpolarizability tensors, $\mathrm{Tr}\Delta\alpha$ is the trace of the polarizability difference between the excited and ground electronic states, $\hat{\mathbf{g}}\cdot\Delta\alpha\cdot\hat{\mathbf{g}}$ is the polarizability change along the transition moment ($\hat{\mathbf{g}}$ is the unit vector), $\Delta\mu_\upsilon$ is the vector change in dipole moment, χ is the angle between the light and electric field vectors, and ξ is the angle between transition dipole moment and $\Delta\mu_\upsilon$ vectors.

Acknowledgment. We gratefully acknowledge the Office of Science, U.S. Department of Energy (Grant DE-FG02-87ER13808), for financial support of the work at Northwestern. The work at the Georgia Institute of Technology was supported by the National Science Foundation (Grant CHE-0342321) and by the IBM Shared University Research Program.

IC050834O

(25) Frisch, M. J.; Trucks, G. W.; Schlegel, H. B.; Scuseria, G. E.; Robb, M. A.; Cheeseman, J. R.; Montgomery, J. A., Jr.; Vreven, T.; Kudin, K. N.; Burant, J. C.; Millam, J. M.; Iyengar, S. S.; Tomasi, J.; Barone, V.; Mennucci, B.; Cossi, M.; Scalmani, G.; Rega, N.; Petersson, G. A.; Nakatsuji, H.; Hada, M.; Ehara, M.; Toyota, K.; Fukuda, R.; Hasegawa, J.; Ishida, M.; Nakajima, T.; Honda, Y.; Kitao, O.; Nakai, H.; Klene, M.; Li, X.; Knox, J. E.; Hratchian, H. P.; Cross, J. B.; Bakken, V.; Adamo, C.; Jaramillo, J.; Gomperts, R.; Stratmann, R. E.; Yazyev, O.; Austin, A. J.; Cammi, R.; Pomelli, C.; Ochterski, J. W.; Ayala, P. Y.; Morokuma, K.; Voth, G. A.; Salvador, P.; Dannenberg, J. J.; Zakrzewski, V. G.; Dapprich, S.; Daniels, A. D.; Strain, M. C.; Farkas, O.; Malick, D. K.; Rabuck, A. D.; Raghavachari, K.; Foresman, J. B.; Ortiz, J. V.; Cui, Q.; Baboul, A. G.; Clifford, S.; Cioslowski, J.; Stefanov, B. B.; Liu, G.; Liashenko, A.; Piskorz, P.; Komaromi, I.; Martin, R. L.; Fox, D. J.; Keith, T.; Al-Laham, M. A.; Peng, C. Y.; Nanayakkara, A.; Challacombe, M.; Gill, P. M. W.; Johnson, B.; Chen, W.; Wong, M. W.; Gonzalez, C.; Pople, J. A. *Gaussian 03*, revision B.05; Gaussian, Inc.: Wallingford, CT, 2004.
(26) Becke, A. D. *J. Chem. Phys.* **1993**, *98*, 5648−5652.
(27) Becke, A. D. *Phys. Rev. A* **1988**, *38*, 3098−3100.
(28) Lee, C.; Yang, W.; Parr, R. G. *Phys. Rev. B* **1988**, *37*, 785−789.
(29) Liptay, W. *Angew. Chem., Int. Ed. Engl.* **1969**, *8*, 177−188.
(30) Liptay, W. Dipole moments and polarizabilities of molecules in excited electronic states. In *Excited* States; Lim, E. C., Ed.; Academic Press: New York, 1974; Vol. 1, pp 129−229.
(31) Karki, L.; Hupp, J. T. *Inorg. Chem.* **1997**, *36*, 3318−3321.
(32) Bublitz, G. U.; Boxer, S. G. *Annu. Rev. Phys. Chem.* **1997**, *48*, 213−242.